Modelling Ion Production inside an Electron Impact Ionizer for High-Vacuum Gas Analysis

J. Emmelkamp[1,*], F.T. Molkenboer[1], H.H.P.Th. Bekman[1], J. van den Brink[1], D.A. Wismeijer[1], N.B. Koster[1], D.J. Maas[1,2], O. Kievit[3], H.A. Lensen[1]

[1]Nano-instrumentation dept., TNO, Delft, The Netherlands

[2]Delft University, Delft, The Netherlands

[3]Semiconductor Equipment dept., TNO, Delft, The Netherlands

[*]Corresponding author: jurjen.emmelkamp@tno.nl

Introduction

Residual Gas Analyzers (RGA) are often used to measure background gases and contaminations in vacuum systems. An ionizer is used to ionize gas molecules and these ions are accelerated and focused by an electrical field from the ion source to form an ion beam. The ions can be discriminated based on mass/charge ratio by a magnetic field, and the selected ions are captured by a detector. The ion charge flux at this detector is measured as a current.

TNO is developing a new kind of contamination analyzer for high-vacuum systems for real time detection of contaminants. We rely on commercial available electron impact ion sources to generate the ions. To study the resulting ion beam as a function of partial gas pressure, gas composition, emission current, and source dimensions we developed a 3D COMSOL 5.5 model using the Electrostatics (es) and Charged Particle Tracing (cpt) modules. The main parameters to be studied are the ion energy distribution and the ion production rate. For our system we require a very homogeneous ion energy and maximized ion production for the detection of contaminants at high-vacuum regimes.

System set-up

The ion source used in our current set-up is obtained from Stanford Research Systems (SRS), and used as electron impact ion source for RGA systems, see Figure 1. This paper uses the SRS ion source for the model presented.

Figure 1. SRS electron impact ion source for RGA applications used for the simulation model. The wired structure is the anode cage and the thin round wire around it is the thermionic electron emission filament (cathode). The ion outlet is directed to the upper left corner. Picture taken from www.thinksrs.com.

The ion source consists of a thermionic electron emitting thoria-coated iridium filament, an open wired anode cage, a grounded outer wired cage (not shown in the figure), and an ion extraction hole in a grounded bottom plate. The electrons can ionize molecules by electron impact inside the anode cage. An secondary electron is removed from the molecule and a positive charged ion remains. The secondary electron is absorbed by the anode cage, and the positively charged ion is extracted from the anode cage towards the extraction hole by the electrical field between anode cage and grounded extraction hole plate to form an ion beam. This ion beam is further processed and detected by the RGA apparatus.

Simulation model

The model is shown in Figure 2. For this model COMSOL 5.5 is used, with the modules for Electrostatics (es) and Charged Particle Tracing (cpt). Electrons are emitted by the filament by thermionic emission and these electrons are accelerated by the electrical field towards the anode cage. Because of the open structure of the cage the majority of the electrons will pass the cage leading to ionizations inside the cage. Ions formed inside the cage are accelerated by the electrical field towards the extraction hole, where they will leave the ion source, forming an ion beam. The filament is set to a voltage of 40 V and the anode has a voltage of 110 V. The outer structure of the cylindrical ion source is grounded. The electrons travel through the anode cage with a kinetic energy of 70 eV (110-40), and the ion energy leaving the source is set to 110 eV.

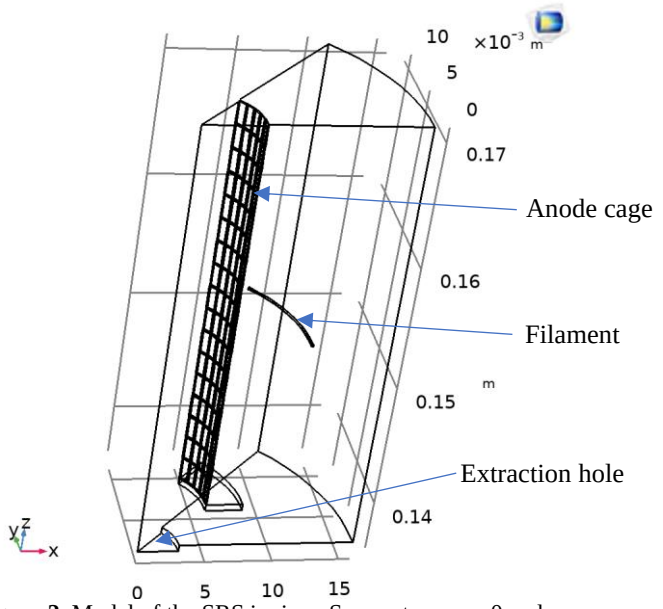

Figure 2. Model of the SRS ionizer. Symmetry on y=0 and y=x. z runs from extraction hole to top of anode cage.

Electric potential

Ions are accelerated towards the extraction hole by the electrical field, and the kinetic energy they obtain equals the potential difference between ionization site and the extraction hole. The latter is grounded, so only the potential at the ionization site dictates the ion energy. For a homogeneous ion energy distribution all ions should be formed at identical potential. The potential field within the anode is shown in Figure 4. It is clear that the majority of the anode cage volume has a fairly homogeneous potential and the only gradient visible is at the bottom of the anode cage near the extraction hole. Space charge by electrons and ions is not taken into account for calculating the potential field since it is expected that they will compensate each other. Negative 'wells' in the potential field caused by the space charge of the electrons will be filled with ions, and the potential will be raised again. Positive 'bumps' in the potential field caused by the space charge of ions will push these ions out by coulomb forces, resulting in flattening of the potential. Therefore a self-regulating effect is expected.

Although the electron space charge is neglected for calculating the electric potential, it is used for estimating the position of the ionization sites. Since the ions are formed by electron impact it is expected that the locations of the ionization sites follow the concentration of the electrons in the anode cage, and the electron space charge is directly coupled to the electron concentration. Charged particle tracing is used to simulate the electron trajectories, and thus for calculating the electron space charge density. The electron flux from the filament is a result of thermionic emission. For the charged particle tracing of the electrons we are interested in the initial electron energy, direction and emission distribution.

Thermionic emission

Thermionic emission is the emission of electrons from a material based on the kT energy of the electrons, and the electron flux can be written as (Orloff, 2008):

$$J(F,T,W) = A_G T^2 e^{\frac{-(W-\Delta W)}{kT}}$$

Where F is the electrical field at the filament surface, T the absolute temperature, W the work function of the filament surface material, ΔW is the Schottky effect or field enhanced thermionic emission, and k is the Boltzmann constant.

$$A_G = \lambda_R A_R$$

λ_R is the material-specific correlation factor that is typically of order 0.5, and A_R is Richardson's constant given by (Crowell, 1965)

$$A_R = \frac{4\pi m k^2 q_e}{h^3} = \frac{4\pi * 9.109\ 10^{-31}\ [kg] * (1.38\ 10^{-23}[J\ K^{-1}])^2 * 1.602\ 10^{-19}\ [C]}{(6.626\ 10^{-34}[J\ s])^3} = 1.20\ 10^6 A\ m^{-2}\ K^{-2};$$

m is the electron mass; q_e is the electron charge; h is the Planck's constant. The estimated Schottky effect equals (Orloff, 2008)

$$\Delta W = \sqrt{\frac{{q_e}^3 F}{4\pi\varepsilon_0}} = \sqrt{\frac{(1.602\ 10^{-19}[C])^3 \frac{110[V]}{(31.75-14.2)[mm]/2}}{4\pi * 8.85\ 10^{-12}[F\ m^{-1}]}} = 6.81\ 10^{-22} J = 4.25\ meV;$$

ε_0 the electric constant (vacuum permittivity). The Schottky effect therefore can be neglected.

Therefore, the only unknown is the work function W. The work function of thoria-coated iridium is unknown, but can be estimated based on the emission current, filament surface area and the filament temperature as given by SRS. SRS states that the filament working temperature is around 1400 °C (SRS, sd), and a common emission current is 1 mA. Based on the dimensions of the filament (estimated radius wire: 0.10 mm; estimated radius filament: 10.7 mm) we find an electron flux from the filament surface of 24 A/m^2 at an emission current of 1 mA. Based on the equation for thermionic emission we find a corresponding work function of ~3.6 eV for λ_R=0.50.

To simulate the electron trajectories we need the initial electron kinetic energy and it's direction. Although it is expected that the electrons are emitted in all directions from the filament, for reasons of simplicity we assume a resulting electron direction normal to the filament surface. Furthermore, the filament is heated by a current running through it, and we assume the filament has a constant thickness and resistance, identical surface temperature is expected over all filament, and thus we expect an even emission distribution over the complete filament surface.

The kinetic energy of an emitted electron is equal to the initial electron energy minus the work function. Only a fraction of all electrons has sufficient energy to overcome the work function, and this fraction is calculated by the exponential function $e^{-\frac{W}{kT}}$. For a work function of 3.6 eV and a temperature of 1670 K, this fraction equals 1.44 10^{-11}. The kinetic energy of the emitted electrons is shown in Figure 3.

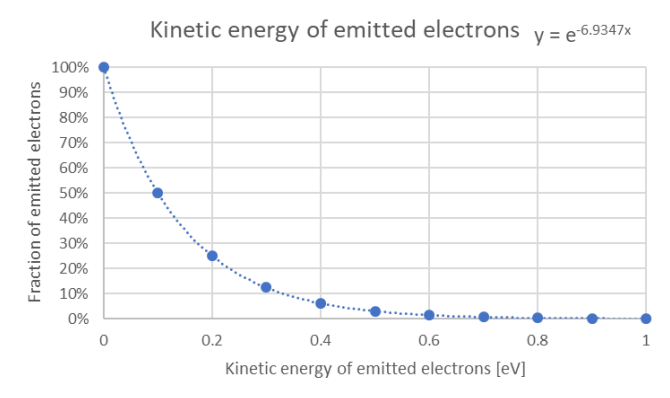

Figure 3. Kinetic energy of emitted electrons for a temperature of 1400 °C and a work function of 3.6 eV for the filament used.

The initial electron energy is given as a function to the electron inlet (filament surface): ekin=1/(-6.9347/log(frac(frac))), where frac is a function with argument frac: frac=0.5+wv1(x). Waveform function wv1 is used as sawtooth without smoothing with an angular frequency of 10π and an amplitude of 0.5.

Ionization rate

Since the ionization itself is not simulated using the model developed, we have to calculate the ionization rate analytically, and use this rate for the model.

The ionization rate can be calculated by the following equation:

$$total\ ionization\ rate = number\ electrons\ passing\ per\ second * \frac{diameter_{anode\ cage}}{electron\ mean\ free\ path}$$

The number of electrons passing per second is the product of the average number of an electron passing the anode cage before it is absorbed by the anode cage and the filament emission current divided by the elementary charge. The number of passes per electron depends on the open fraction of the anode cage. For the first pass an electron needs to penetrate one open mesh, but for every next pass it needs to penetrate the open mesh twice, reducing the chances for a successful pass. We estimate the wire fraction at 10% for both the horizontal and vertical wires, resulting in an open fraction of 81%, leading to an average number of passes per electron of 2.35. For an emission current of 1 mA the number of electrons passing per second becomes $3.3\ 10^{16}$.

The diameter of the anode cage is measured at 15 mm and the electron mean free path can be calculated as:

$$Electron\ mean\ free\ path_M = \frac{k_B T}{\sqrt{2} p_M \sigma_M}$$

With k_B is the Boltzmann constant, T the absolute temperature, p_M the partial pressure of the gas with molecule mass M and σ_M the ionization cross section of this gas. The ionization cross section can be estimated based on the ionization cross section of xenon:

$$\sigma_M \sim \sigma_{Xe} \left(\frac{M_M}{M_{Xe}}\right)^{2/3}$$

where $\sigma_{Xe} = 5.4\ 10^{-20}\ m^2$ (E=70 eV) (Biagi, 2020). For xenon (M=131, taken as average over the major 7 isotopes) as reference the electron mean free path at a pressure of $1.0\ 10^{-6}$ mbar and a temperature of 310K is around 0.79 km.

It is expected that ionization is evenly distributed over the complete cross section length, because the ionization chance is almost constant for the electrons traveling through the anode cage, since the electron free path length is expected to be around 1 km, which is infinitely long compared to the anode diameter. For reasons of simplicity scattering of electrons at the anode wires is neglected.

The total ionization rate equals:

$$total\ ionization\ rate = number\ electrons\ passing\ per\ second * \frac{dia_{anode\ cage}}{electron\ mean\ free\ path}$$

$$= 1.5\ 10^{16}\ s^{-1} * \frac{15mm}{0.79\ km} = 2.8\ 10^{11}\ s^{-1}$$

Study sequence

The study sequence consists of 4 steps:

Step	Type	Physics	Times	Outcome
1	Stationary	Electrostatics (es)		Electric potential.
2	Time dependent	Charged Particle Tracing (cpt)	range(0,10e-10,10e-8)	Electron trajectories, electron space charge density.
3	Stationary	Electrostatics (es1)		Electric potential and electron space charge density required for ion energy distribution.
4	Time dependent	Charged Particle Tracing (cpt1)	range(0,3e-6,3e-4)	Ion trajectories.

Simulation results

The simulation results will be treated according to the step sequence as shown in the table above.

Electric potential

In the first step the electric potential is calculated, see Figure 4. Anode is set to 110 V, filament to 40 V and outer cage is grounded. The electrical potential shows great homogeneity over almost the complete ion source. Only a small drop in potential near the extraction hole is observed. Homogeneous ion energy is expected.

Electron trajectories

1000 electron trajectories are modeled, and the decay of the electrons available for ionization is shown in Figure 5. Due to absorption by the anode grid and the filament itself, there is a decay in remaining electrons. Plots of the trajectories at 3 different emission times are shown in Figure 6.

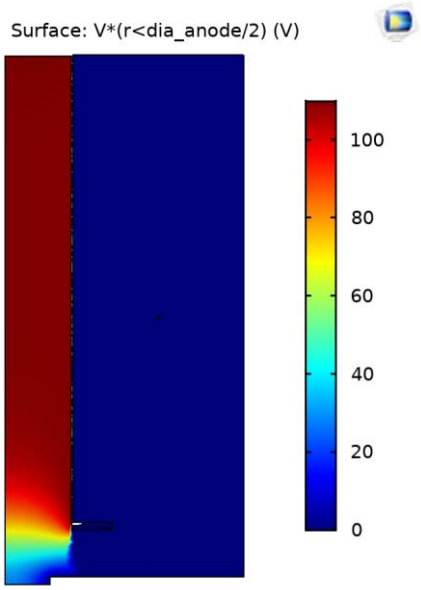

Figure 4. Potential field inside anode cage indicating the kinetic energy ions will obtain when produced at a specific location.

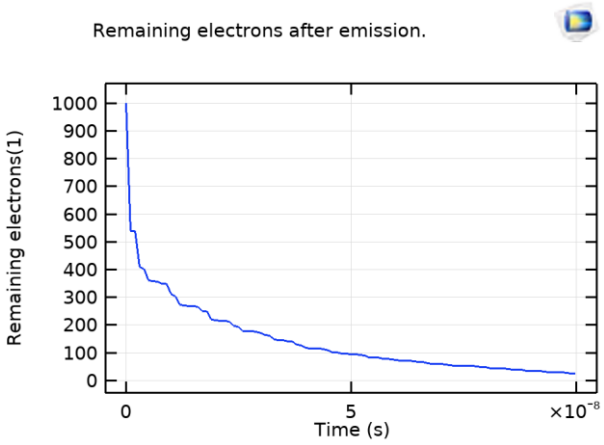

Figure 5. Decay of electrons after emission from the filament. First immediate drop is the decay by absorption by the filament itself. Further drops are due to absorption by the anode.

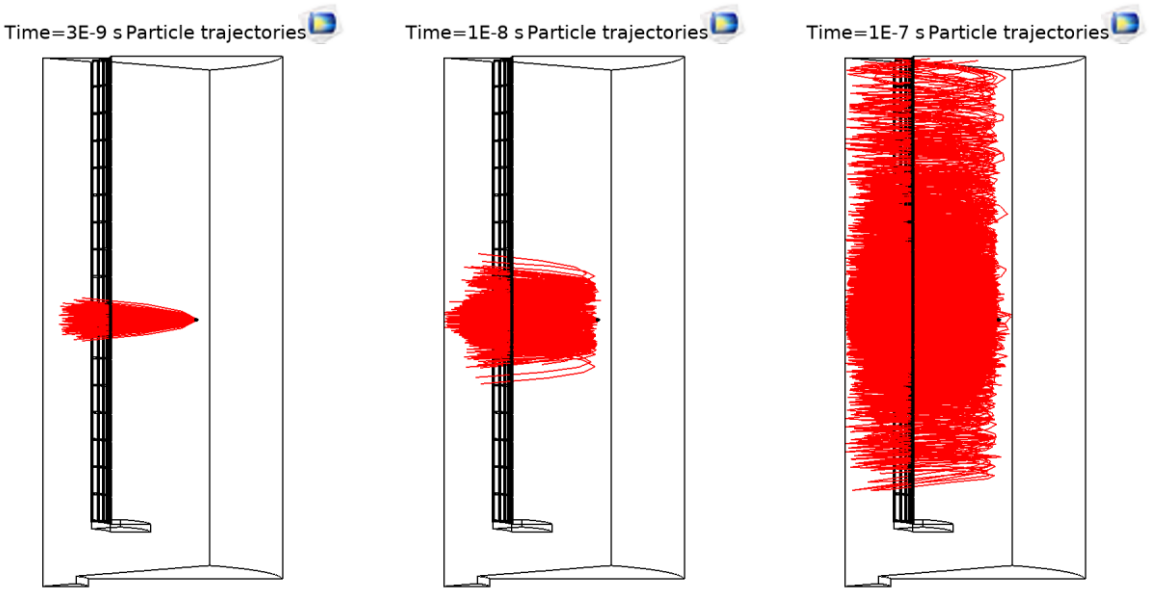

Figure 6. Electron trajectories after release from the filament. Three different release times: 3 ns (left, just before the electrons have reached the center axis), 10 ns (middle, just before the electrons have reached the center axis for the second time) and 100 ns (right).

Electron space charge density and ion energy

The release of ions is based on the electron space charge density. The electron space charge density after >90% of the electrons available for ionization at t=100 ns is shown in Figure 7. A histogram function over the potential inside the anode cage indicates the ion energy distribution, see Figure 8. Clearly visible is the strong peak at 109 eV, although the cumulative shows that ion energies outside this peak cannot be completely neglected.

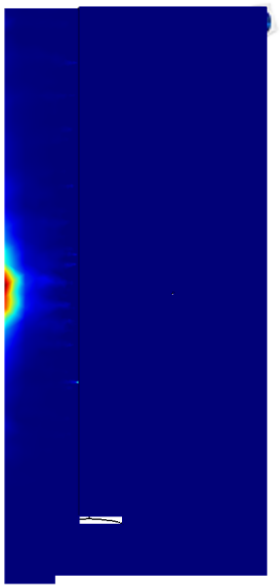

Figure 7. Electron space charge density inside anode cage indicating ionization sites.

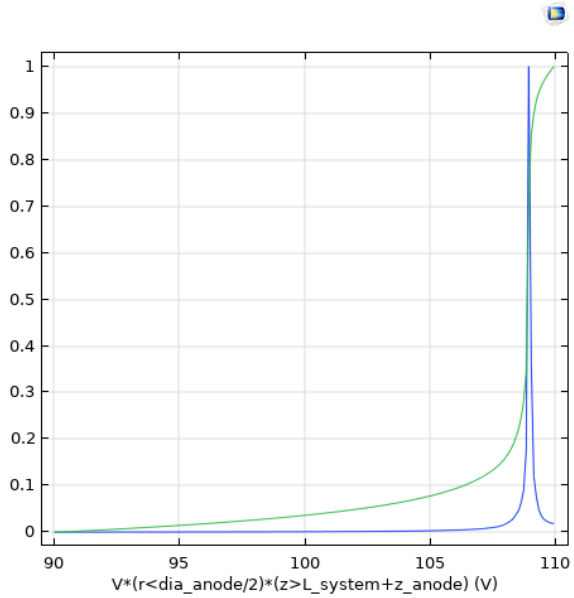

Figure 8. Ion energy distribution (blue line) and its cumulative (green line).

Ionization sites

The ionization site distribution and ion trajectories are shown in Figure 9 and Figure 10, resp.

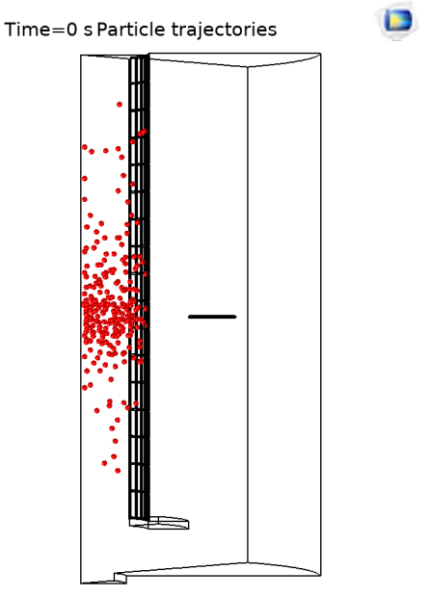

Figure 9. Ionization positions (N=1000) based on the electron space charge density.

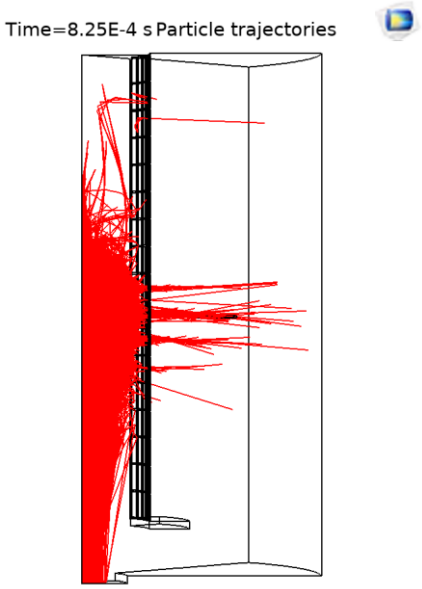

Figure 10. Ion trajectories after ionization.

Some ions formed close to the anode grid openings can escape from the anode cage due to local electrical field lines pointing through the grid openings outwards. However, the majority of the ions leave the source via the extraction hole. Clearly visible is that the ions exit the source close to the center line, all within half of the radius. Due to the homogeneous electric potential the ions experience only a very small acceleration force after formation, and time is needed for the release, in the millisecond range, see Figure 11. Only little over 50% of the released ions are extracted from the source. The reason of this low percentage has probably to do with the mesh being too coarse, and ions can falsely reach the anode. The ion beam intensity at the extraction hole is plotted in Figure 12. The small diameter of the intense part of the ion beam is clearly visible, and the complete radius of the ion beam is around one-third of the radius of the extraction hole. However, a finer mesh will be required for more reliable results.

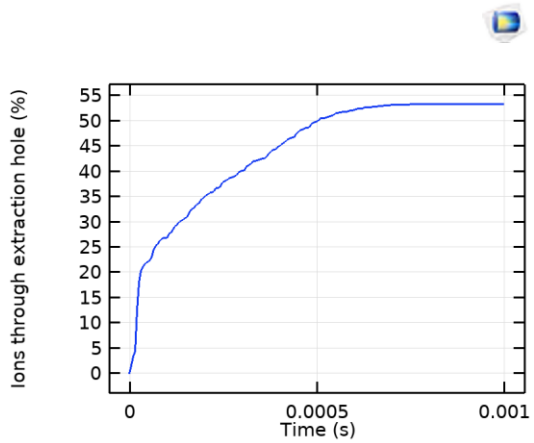

Figure 11. Ions collected at extraction hole.

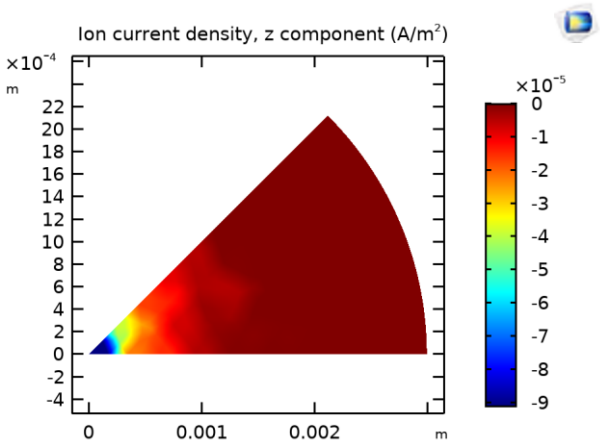

Figure 12. Ion beam intensity at the extraction hole.

Experimental validation

At this very moment we are working on the quantitative experimental validation of the ion beam produced by the SRS ion source, however, no reliable results have been obtained yet. The measured ion currents showed too low readings, probably due to the detector used. Severe scattering at the detector is expected. Qualitative ion beam measurements by use of a phosphor screen are planned.

Conclusions

A 3D multistep Multiphysics COMSOL model was developed that can estimate the ion energy distribution of an electron impact ion source for high-vacuum systems. Also the produced diameter and intensity profile of the ion beam can be estimated, and thus the ion flux. The ion beam appears to be very narrow with high intensity in the very middle. Mesh refinement is required to obtain better predictions. Qualitative and quantitative experiments for validation are in progress.

Acknowledgements

This project has received funding from the ECSEL Joint Undertaking (JU) under grant agreement No 826589. The JU receives support from the European Union's Horizon 2020 research and innovation programme and France, Germany, Austria, Italy, Sweden, Netherlands, Belgium, Hungary, Romania, Israel.

References

Biagi, S. (2020, September 17). *MagBoltz v8.97 database, Fortran program*. Retrieved from LxCat: www.lxcat.net

Crowell, C. (1965). The Richardson constant for thermionic emission in Schottky barrier diodes. *Solid-State Electronics 8 (4)*, 395-399.

Orloff, J. (2008). Schottky emission. In *Handbook of Charged Particle Optics (2nd ed.)* (pp. 5-6). CRC Press.

SRS. (n.d.). *Application notes*. Retrieved from ThinkSRS: https://www.thinksrs.com/downloads/pdfs/applicationnotes/IG1filamentsapp.pdf